Finite Element Analysis of the Axially Non-symmetrical Piercing Punches Performance for Belt Perforation

Dominik Wojtkowiak[0000-0003-1334-1288] and *Krzysztof* Talaśka[0000-0001-9736-9725]

Poznan University of Technology, Institute of Machine Design, Piotrowo 3, 61-138 Poznań, Poland

Abstract. Modification of the punch geometry can greatly reduce the force necessary to perform the perforation of the belt. This paper presents research on axially non-symmetrical piercing punches – double sheared one and one with a cylindrical bowl. FEM analysis was performed for a variable tip angle β in the 60-150° range for a double sheared punch or a variable bowl radius R in the 5.25-10 mm range and for a constant punch diameter D = 10 mm and TFL10S belt. Based on the obtained results, the influence of the tip angle β (for the double sheared punch) and the bowl radius R (for a cylindrical bowl punch) on the perforation force F_P and pneumatic cylinder stroke increase Δs was determined. FEM analysis was used to obtain the perforation force in function of punch displacement characteristics for various tool geometry. Based on the results, the characteristics of the perforation force in function of punch geometrical parameters were determined. Additionally, their application in the punching die design process, where the effective geometrical features of the tools are desired, is presented.

1 Introduction

Modification of the punch geometry can greatly reduce the force necessary to make a hole in the material [1-4]. One of the methods is to create an axially non-symmetrical tool by either performing the symmetrical shearing of the cylindrical punch (a double sheared punch – Fig. 1a) [5-8], or milling the cylindrical bowl in the punch front surface (a cylindrical bowl punch – Fig. 1b) [5-8]. Their positive effect was proved for metal punching [5], but for multilayer polymer composite belts (Fig. 2) their performance was not tested.

Belt punching with using two cutting edges (the punch and the die) is rather a complex issue. Because of the orthotropic mechanical properties of the polymer multilayer composite belts, the classical theory used in punching is not always applicable in such cases. Some correlations can be discovered in the behavior of non-classical materials [9-11] or natural polymers [12, 13]. Not only the mechanical properties, but also the chemical compound [14] or thermomechanical properties [15-17] can affect the course of the machining process.

The objective of the presented research is to find the influence of the tip angle β on the perforation force F_P and pneumatic cylinder stroke increase Δs. This information can be useful during the design process of punching dies for belt perforation. By applying the restrictions connected with the design assumptions, it is possible to perform the optimization of the tool geometry and, as a result, achieve the effective construction of the machine. These parameters have an impact on selecting proper drive [18, 19] and positioning method [20, 21], which also affects the efficiency of the process [22].

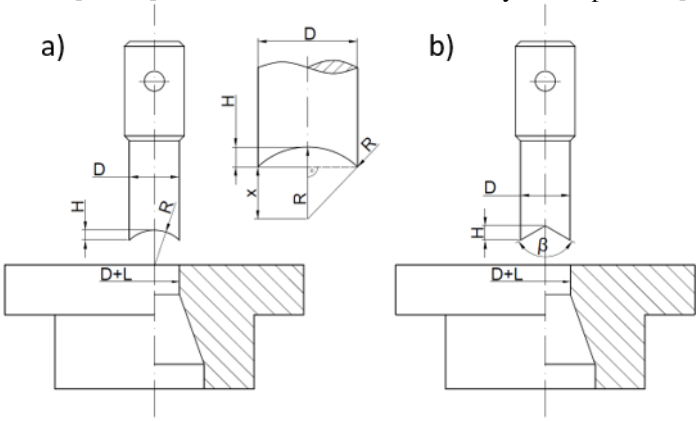

Fig. 1. Axially non-symmetrical punchescooperating witha die a) double sheared punch, b) cylindrical bowl punch: D –punch diameter, H – shearing/bowl height, L – punch-die clearance, β – tip angle, R – bowl radius.

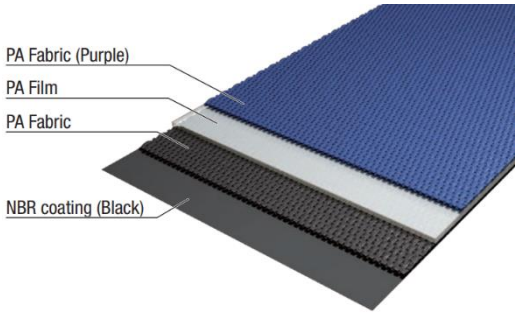

Fig. 2. Multilayer polymer composite belt [23].

2 Methodology of research

The main part of the research was FEM analysis performed in ABAQUS. It is very often used to improve the design of the machines [24-26] as well as the manufacturing process [27-29].The clear advantage of using FEA is that there is no necessity to make a set of tools with various shapes [1-3, 30, 31]. However, to verify the correctness of the developed model at least one experimental result is required to compare it with the computer simulation results. The results of the experimental tests were obtained from [1].

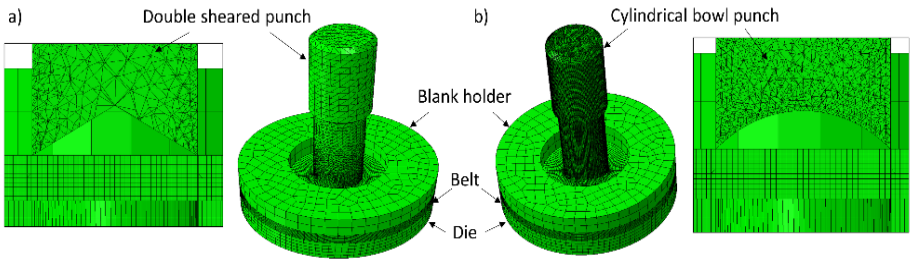

Fig. 3. FEM model construction.

In the used ABAQUS Explicit model, the belt is modelled as a deformable part, while the rest of the components (punch, die and blank holder) are defined as rigid objects, which is justified since the stiffness of the belt is much smaller than the steel tools. The kinematic extortion of the punch was specified as the boundary condition with the velocity in the Z axis of 0.5 mm/s. Using low velocity provides a quasi-static characteristic of the analyzed process, which makes the influence of the strain rate negligible and enables using mass scaling without affecting the results. The obtained results are in the form of reaction force in the reference point of the punch ($F_P(t)$). To adjust the moment of belt failure, the damage evolution has to be defined by using proper displacement at failure. Because variable punch geometry affects the mesh, which has an impact on this parameter, it has to be established for each single analysis. Based on the observation of the test punching process, the failure should occur when the inner edge in the side view meets the cutting edge of the die.
The tests were conducted for the TFL10S belt, whose construction is very similar to the one presented in Fig. 2, but the top layer is also covered with NBR rubber. This type of belt is characterized with increased strength and high rigidity. This makes it is hard to perforate and a reasonable choice as the test material. Its thickness equals t = 2.65 mm, while the polyamide core inside its structure is 1 mm thick. The parameters used to model the belt properties and its damage in the FEM model are presented in Table 1 and were determined based on the previous research [1, 2]. Although the belt should be considered an orthotropic material, during FEM analysis the isotropic substitute parameters and Johnson-Cook damage model were used. This simplification is explained and justified in [1, 2, 32].

Table 1. Mechanical properties of the TFL10S belt used for FEM modelling.

Density ρ [kg/m^3]	Young's Moduli E[MPa]	Poisson ratio v[-]	Johnson-Cook model parameters				
			d_1	d_2	d_3	d_4	d_5
1140	235	0.2	-0.24	0.32	2.6	0	0

To determine the test range of the variable tip angle, the correlation between the geometrical parameters of the punch and the tip angle β was specified (Fig. 1a):

$$tan\left(\frac{\beta}{2}\right) = \frac{D}{2H} \rightarrow \beta = 2 \cdot tan^{-1}\left(\frac{D}{2H}\right) \qquad (1)$$

In order to maintain the constant mechanical cutting work during the process and prevent the closed-contour punching to obtain the most effective force reduction, we can assume that the shearing height H should be greater or equal to the belt thickness t. For a punch

with diameter D = 10 mm, the maximum tip angle β should be lower than 124°. Based on that, in this research two tip angles over this value and a few lower than the estimated value are considered. Tests were performed for tip angles β = 60°, 90°, 105°, 120°, 135° and 150°.

The same methodology of determining the test range of bowl radius R was usedfor a cylindrical bowl punch. In this case, the correlation between the geometrical features, presented in Fig. 1, can be described with equations 2-4. Applying the $H = t$ into the final equation provides information that the bowl radius should be at most 6.04 mm. Due to the technological reasons, the punch bowl radius R should equal the milling tool radius. Additionally, it is impossible to machine bowl with radius R lower or equal $½D$. All these facts were used to establish the following test values of bowl radius R for research: R = 5.25, 5.5, 6, 6.5, 7.25, 8 and 10 mm.

$$x^2 + \left(\frac{D}{2}\right)^2 = R^2 \rightarrow x = \sqrt{R^2 - \frac{D^2}{4}} \tag{2}$$

$$H + x = R \rightarrow x = R - H \tag{3}$$

$$R - H = \sqrt{R^2 - \frac{D^2}{4}} \rightarrow R = \frac{H}{2} + \frac{D^2}{8H} \tag{4}$$

3 Results and discussion

The comparison of the FEM and experimental results for TFL10S belt perforation with a double shear punch with a tip angle β = 120° is presented in Fig. 4. As can be observed, the divergence of the characteristics is significant. The main difference is connected with the damage of the material, which is very soft in the experimental curve and sudden in the FEM one. It is caused by the isotropic approach and impossibility of modelling the hardening caused by the polyamide core. However, the peak value does not lie too far from the experimental one – for FEM F_{PMAX} = 3429 N and for experimental tests F_{PMAX} = 3507 N. This indicates that the proposed model is not appropriate for the force characteristic approximation and can be just used for the estimation of the peak force tendency for various tool geometry. The similar explanation can be used for the comparison of the FEM and experimental results for TFL10S belt perforation with a cylindrical punch with bowl radius R = 7.25 mm (Fig. 5). However, in this case the characteristics are much more similar to each other (experimental value F_{PMAX} = 2568 N, FEM value F_{PMAX} = 2123 N) due to the almost symmetrical characteristics of the force increase and decrease, but still the fracture of the belt is also rupture.

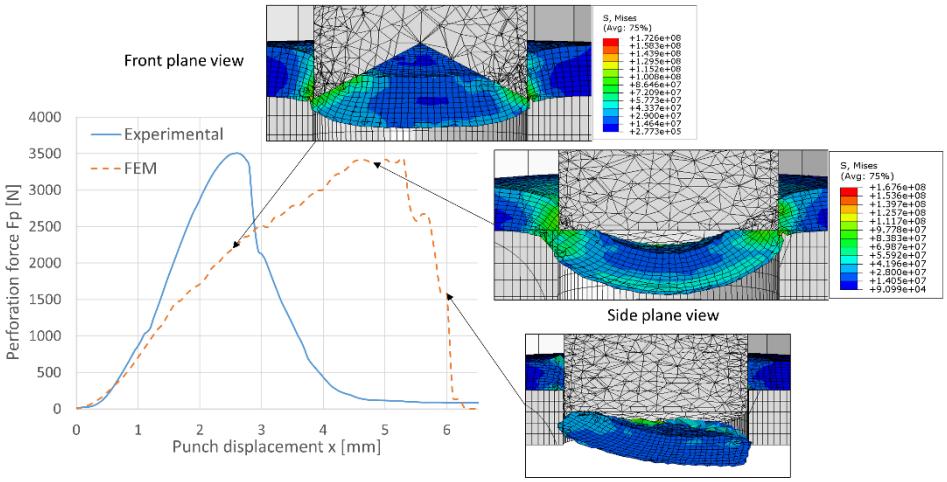

Fig. 4. Comparison of FEM and experimental results for TFL10S belt perforation with a double shear punch with a tip angle $\beta = 120°$ along with sample stress distribution obtained from FEM analysis.

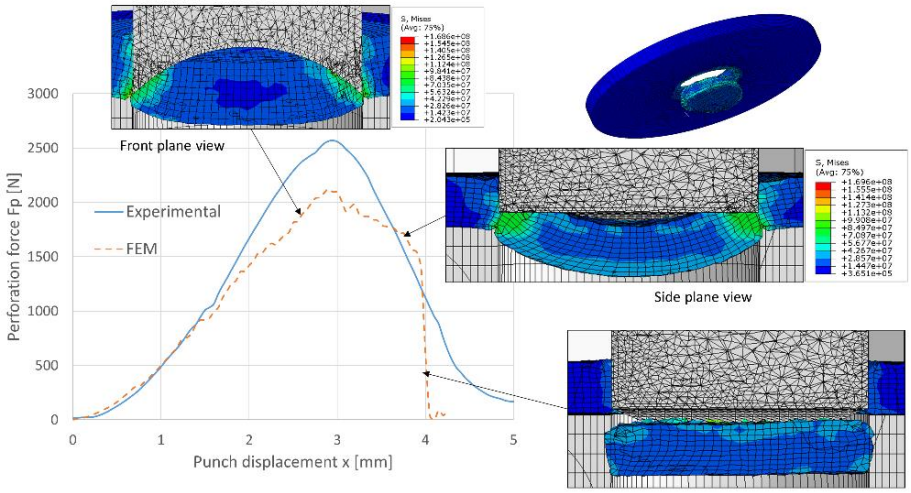

Fig. 5. Comparison of FEM and experimental results for TFL10S belt perforation with a cylindrical bowl punch with bowl radius $R = 7.25$ mm along with sample stress distribution obtained from the FEM analysis.

The results are presented in Tables 2 and 3. Based on these results, the characteristics show the influence of the main geometrical parameters (tip angle β and bowl radius R) on the perforation force F_P, for both types of axially non-symmetrical piercing punches (Fig. 6).

Table 2. Results of FEM analysis of the double sheared punch during TFL10S belt perforation.

Tip angle β [°]	Perforation force F_P [N]	Stroke increase Δs [mm]
60	985	8.66
90	1981	5
105	3380	3.83
120	3429	2.89
135	3828	2.07
150	4201	1.34

Table 3. Results of FEM analysis of the cylindrical bowl punch during TFL10S belt perforation.

Bowl radius R [mm]	Perforation force F_P [N]	Stroke increase Δs [mm]
5.25	1452	3.64
5.5	1503	3.21
6	1533	2.68
6.5	1599	2.35
7.25	2123	2
8	2348	1.76
10	2523	1.34

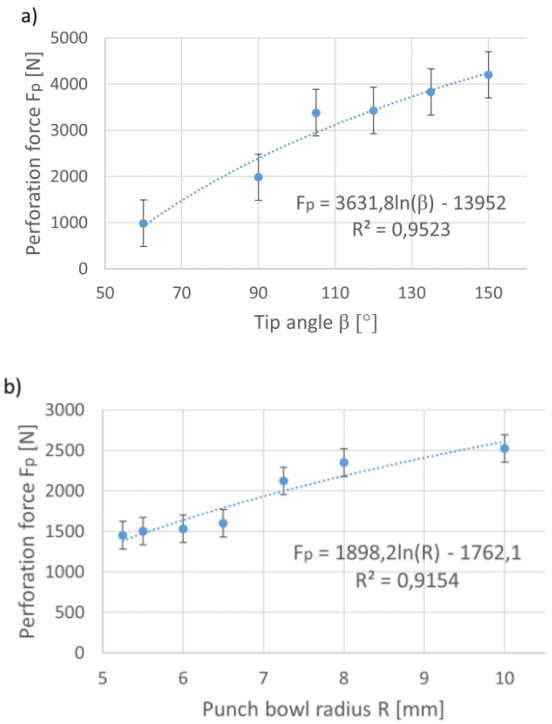

Fig. 6. The influence of the tip angle β (a) and bowl radius R (b) on the perforation force F_P for axially non-symmetrical piercing punches.

As can be observed, there is a positive exponential correlation between the tip angle β or the bowl radius R and the perforation force F_P. It indicates that we should use the highest possible values. However, it will greatly increase pneumatic cylinder stroke Δs necessary to perform the work. Additionally, sharpening the cutting edges of the axially non-symmetrical piercing punch will decrease the tool life. In order to gain the effective solution, it is required to find a compromise between these parameters. Additionally, it is worth mentioning that the scrap and the hole (Fig. 5) are much more deformed than for the axially symmetrical punches, which means that the quality of the holes may be decreased.

4 Summary

Based on the obtained results, we can conclude that using axially non-symmetrical piercing punches can reduce the perforation force, without generating additional transverse force, which causes punch deflection. But compared to the axially symmetrical punches (e.g. spherical bowl punches), they still cause some issues (ovality of the hole, stroke increase etc.). In order to obtain the effective reduction of the perforation force F_P, the tip angle should be lower than 124°or the bowl punch should have radius R lower than 6 mm in order to avoid closed-contour punching. Based on the presented characteristics, it is possible to find an effective solution which fulfills design criteria. It demonstrates that axially non-symmetrical punches are appropriate for belt perforation, but in a limited range.

References

1. D. Wojtkowiak, K. Talaśka, I. Malujda, G. Domek Estimation of the perforation force for polymer composite conveyor belts taking into consideration the shape of the piercing punch. Int J AdvManufTechnol 98, 9-12, 2539–2561 (2018).
2. D. Wojtkowiak, K. Talaśka Determination of the effective geometrical features of the piercing punch for polymer composite belts. Int J Adv Manuf Technol 104, 1-4, 315–332 (2019).
3. D. Wojtkowiak, K. Talaśka, D. Wilczyński Evaluation of the belt punching process efficiency based on the resistance force of the compressed material, Int J Adv Manuf Technol, DOI: 10.1007/s00170-020-05819-4 (2020).
4. D. Wojtkowiak, K. Talaśka, I. Malujda, G. Domek Analysis of the influence of the cutting edge geometry on parameters of the perforation process for conveyor and transmission belts. MATEC Web of Conferences, 157, 01022 (2018).
5. U.P. Singh, A.H. Strepel, H.J.J Kals Design study of the geometry of a punching/blanking tool. J Mat Process Technol 33, 331–345 (1992).
6. Choosing the Right Shear for Your Application. http://www.fabricatingandmetalworking.com - access 07.07.2020.
7. Punch press tooling. http://www.theartofpressbrake.com - access 07.07.2020.
8. Wilson High Performance™ Fab Toolingfor Thin Turretstrippit® Machines. https://www.wilsontool.com - access 07.07.2020.
9. J. Górecki, I. Malujda, K. Talaśka Influence of the Value of Limit densification Stress on the Quality of Pellets During the Agglomeration Process of CO_2. Procedia Engineering, 136, 269-274 (2016).
10. J. Górecki, I. Malujda, K. Talaśka K., et al. Dry ice compaction in piston extrusion process. Acta Mechanica et Automatica, 11, 4, 313-316 (2017).

11. J. Górecki, K. Talaśka, K. Wałęsa, D. Wilczyński, D. Wojtkowiak Mathematical Model Describing the Influence of Geometrical Parameters of Multichannel Dies on the Limit Force of Dry Ice Extrusion Process. Materials, 13, 15 (2020).
12. I. Malujda, D. Wilczyński Mechanical properties investigation of natural polymers. Procedia Engineering, 136, 263-268 (2016).
13. K. Talaśka, I. Malujda, D. Wilczyński Agglomeration of natural fibrous materials in perpetual screw technique - a challenge for designer. Procedia Engineering, 136, 63-69 (2016).
14. P. Krawiec, M. Pajtášová, F. Meler, Ł. Warguła Testing functional features of V-belt transmissions. IOP Conferences: Materials Science and Engineering, 776, 012008 (2020).
15. K. Wałęsa, I. Malujda, D. Wilczyński Experimental research of the thermoplastic belt plasticizing process in the hot plate welding. IOP Conferences: Materials Science and Engineering, 776, 1, 012011 (2020).
16. K. Wałęsa, I. Malujda, J. Górecki Experimental research of the mechanical properties of the round drive belts made of thermoplastic elastomer. IOP Conferences: Materials Science and Engineering, 776, 1, 012107 (2020).
17. K. Wałęsa, I. Malujda, D. Wilczyński Shaping the parameters of cylindrical belt surface in the joint area. ActaMechanica et Automatica, 13, 4, 255-261 (2019).
18. M. Kukla, P. Tarkowski, I. Malujda, K. Talaśka, J. Górecki Determination of the torque characteristics of stepper motor. Procedia Engineering, 136, 375-379 (2016).
19. A. Fierek, I. Malujda, K. Talaśka Design of a mechatronic unit for application of coats of adhesive. MATEC Web of Conferences, 254, 01019 (2019).
20. Ł. Magdziak, I. Malujda, D. Wilczyński, D. Wojtkowiak Concept of improving positioning of pneumatic drive as drive of manipulator. Procedia Engineering, 177, 331-338 (2017).
21. P. Perz, I. Malujda, D. Wilczyński, P. Tarkowski Methods of controlling a hybrid positioning system using LabVIEW. Procedia Engineering, 177, 339-346 (2017).
22. P. Tarkowski, I. Malujda, K. Talaśka, J. Górecki, M. Kukla Influence of the type of acceleration characteristic of the stepping motor for efficient power usage. Procedia Engineering, 136, 370-374 (2016).
23. PolyBeltTM for Printing Machine and Book Binding Machine. www.nitta.de - access 07.07.2020.
24. A. Fierek, I. Malujda, D. Wilczyński, K. Wałęsa Analysis of shaft selection in terms of stiffness and mass. IOP Conference Series: Materials Science and Engineering, 776, 012028 (2020).
25. D. Wojtkowiak, K. Talaśka, A. Fierek The application of the Finite Element Method analysis in the process of designing the punching die for belt perforation, IOP Conferences: Materials Science and Engineering, 776, 012057 (2020).
26. D. Wojtkowiak, K. Talaśka, M. Berdychowski Analysis of the guiding column and sleeve cooperation in the linear slide bearing of the punching die head-punch block. IOP Conferences: Materials Science and Engineering, 776, 012055 (2020).
27. M. Berdychowski, J. Mielniczuk Analysis of the porous bone-implant fixation-experimental verification of numerical model. MATEC Web of Conferences, 157, 05002 (2018).
28. M. Berdychowski, J. Mielniczuk, M. Matyjaszczyk Analysis of the Yield Condition of Porous Bone-implant Fixation. Procedia Engineering, 177, 358-362 (2017).
29. M. Berdychowski, D. Wilczyński, K. Wałęsa, J. Górecki Research on the compaction process of loose materials with use of helix technology. IOP Conference Series: Materials Science and Engineering, 776, 012063 (2020).
30. D. Wojtkowiak, K. Talaśka The influence of the piercing punch profile on the stress distribution on its cutting edge. MATEC Web of Conferences, 254, 02001 (2019).

31. D. Wojtkowiak, K. Talaśka Modelling the Belt Perforation Process with the Piercing Punch and the Die in Context of the Construction of the Punching Dies, IOP Conferences: Materials Science and Engineering, 647, 012013 (2019).
32. K. Talaśka, D. Wojtkowiak Modelling a mechanical properties of the multilayer composite materials with the polyamide core. MATEC Web of Conferences, 157, 02052 (2018).